

We are IntechOpen, the world's leading publisher of Open Access books Built by scientists, for scientists

4,800

Open access books available

122,000

International authors and editors

135M

Downloads

Our authors are among the

154

Countries delivered to

TOP 1%

most cited scientists

12.2%

Contributors from top 500 universities



WEB OF SCIENCE™

Selection of our books indexed in the Book Citation Index
in Web of Science™ Core Collection (BKCI)

Interested in publishing with us?
Contact book.department@intechopen.com

Numbers displayed above are based on latest data collected.

For more information visit www.intechopen.com



Porphyrin Based Dye Sensitized Solar Cells

Matthew J. Griffith and Attila J. Mozer

ARC Centre of Excellence for Electromaterials Science and Intelligent Polymer Research
Institute, University of Wollongong, Squires Way, Fairy Meadow, NSW,
Australia

1. Introduction

Dye-sensitized solar cells (DSSCs) have emerged as an innovative solar energy conversion technology which provides a pathway for the development of cheap, renewable and environmentally acceptable energy production (Gledhill, Scott et al., 2005; O'Regan & Grätzel, 1991; Shaheen, Ginley et al., 2005). A typical DSSC consists of a sensitizing dye chemically anchored to a nanocrystalline wide band gap semiconductor, such as TiO₂, ZnO or SnO₂. The oxide structure is mesoporous in order to produce a high surface area for dye coverage, allowing the adsorbed monolayer to capture the majority of the incident solar flux within the dye band gap. The porous photoanode is immersed in an electrolyte which contains a redox mediator to transport positive charge to the counter electrode and maintain net electrical neutrality (Figure 1). Efficient charge separation is achieved through photoinduced electron injection from the excited state of the sensitizing dye into the conduction band of the metal oxide semiconductor. The resulting dye cations are subsequently reduced by the redox electrolyte, which also conducts the holes to the platinum-coated cathode. The solar to electric power conversion efficiencies of DSSCs depend on a delicate balance of the kinetics for injection, dye regeneration and recombination reactions (Haque, Palomares et al., 2005), with the best devices, currently based on ruthenium polypyridyl sensitizers and an iodide/triiodide redox mediator, exhibiting certified power conversion efficiencies of over 11% (Chiba, Islam et al., 2006).

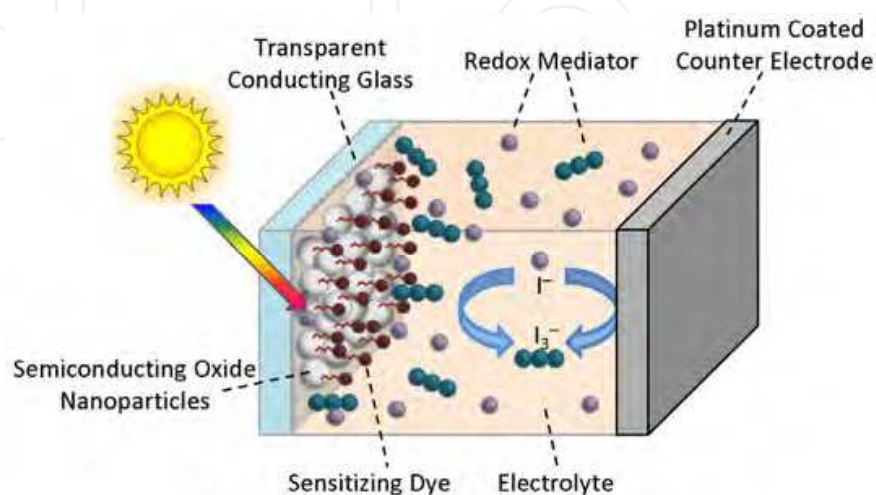


Fig. 1. Schematic illustration of a typical dye-sensitized solar cell (DSSC).

Porphyrin dyes have attracted significant interest as alternative sensitizers in DSSCs due to advantages with moderate material costs, ease of synthesis, large extinction coefficients and high stabilities. However, these dyes present a unique challenge since they have been found to possess very different operational photophysics to the majority of other sensitizing agents. Accordingly, porphyrin sensitizers create the opportunity to study some of the most fundamental limiting factors of DSSCs. In this chapter we will provide a detailed overview of the distinctive properties of porphyrin molecules and their behaviour as sensitizers in DSSCs. We focus on the major limitations affecting the performance of porphyrin DSSCs, including light harvesting, electron injection and charge recombination affects. We will also examine several strategies that have been employed to circumvent these limitations.

1.1 Operational principles of DSSCs

Unlike traditional silicon-based photovoltaic devices, charge separation and recombination in DSSCs are exclusively interfacial reactions. Furthermore, the initial photoexcited species in organic molecules are very different from those of silicon. Since organic molecules have lower dielectric constants and weaker Van der Waals interactions between molecules than their silicon counterparts, photoexcitation of organic dyes produces a tightly bound neutral Frenkel exciton. This is in contrast to the loosely bound Werner excitons produced when silicon is photoexcited, which can essentially be considered free charges. Accordingly, DSSCs require an additional charge separation step to generate free charges. The viability of DSSCs for efficient photovoltaic energy conversion therefore relies almost entirely on achieving a delicate kinetic balance between the desired electron injection and dye cation regeneration reactions and the undesirable recombination reactions with either the dye cations or the acceptor species in electrolyte. The free energy driving forces for these various reactions are therefore crucial in determining the operational efficiency of DSSCs. These driving forces are often indicated by potential energy diagrams such as Figure 2, although such descriptions neglect entropy affects and thus do not strictly represent free energy.

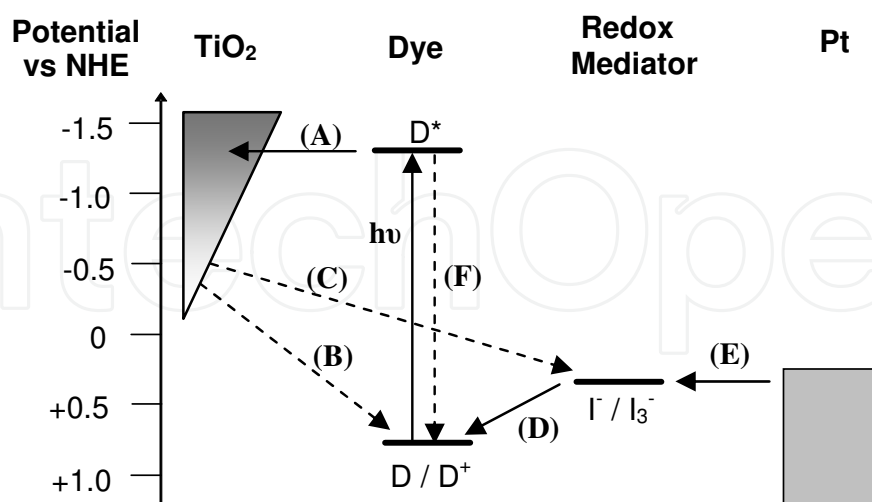


Fig. 2. Schematic representation of the energy levels of a DSSC indicating competing photophysical pathways, including (A) electron injection, (B) electron recombination with dye cations and (C) with the acceptor species in the electrolyte, (D) regeneration of dye cations by I^- , and (E) recycling of I_3^- at the counter electrode. Figure taken from (Wagner, Griffith et al., 2011) and reproduced by permission of The American Chemical Society.

Current generation in the DSSC is dependent on three independent processes; the absorption of light by the photosensitizer, the injection of electrons from the excited photosensitizer, and the charge transport through the semiconductor film. The incident photon-to-current conversion efficiency (IPCE), also referred to as the external quantum efficiency (EQE), which corresponds to the electron flux measured as photocurrent compared to the photon flux that strikes the cell, is simply a combination of the quantum yields for these three processes as expressed in Equation 1.

$$IPCE(\lambda) = LHE(\lambda) \phi_{inj} \eta_{coll} \tag{1}$$

Here $LHE(\lambda)$ is the light harvesting efficiency for photons of wavelength λ , ϕ_{inj} is the quantum yield for electron injection and η_{coll} is the electron collection efficiency. The short circuit current density (J_{sc}) achieved by the device is simply the integrated overlap between the IPCE spectrum and the solar irradiance spectrum ($I_0(\lambda)$) over all wavelengths:

$$J_{sc} = \int q I_0(\lambda) IPCE(\lambda) d\lambda \tag{2}$$

The photovoltage generated by a DSSC is given by the difference in the Fermi energy, E_F , of electrons at the two contacts. Under electrochemical equilibrium in the dark, E_F must be equal for all components of the DSSC. Since the density of states in the semiconductor is not large enough to appreciably affect $E_{F,redox}$, the redox mediator Fermi level, the dark Fermi level is extremely close to $E_{F,redox}$. At open circuit and under illumination, the concentration of electrons in the TiO_2 film increases to a steady state value, n_{light} , determined by the balance of electron injection and recombination. The photovoltage, V_{photo} which corresponds to the increase in the electron Fermi level, is therefore determined by the ratio of the free electron concentration in the TiO_2 under illumination and in the dark:

$$V_{photo} = \frac{1}{q} (E_F - E_{F,Redox}) = \frac{K_B T}{q} \ln \frac{n_{light}}{n_{dark}} \tag{3}$$

The overall power conversion efficiency of a DSSC, η_{global} , is then determined from the intensity of the incident light (I_0), the short circuit current density (J_{sc}), the open-circuit photovoltage (V_{oc}), and the fill factor of the cell (FF) (which is simply the ratio of the maximum power obtained from a device to the theoretical maximum $J_{sc} V_{oc}$):

$$\eta_{global} = \frac{J_{sc} V_{oc} FF}{I_0} \tag{4}$$

The maximum value of η_{global} which can be obtained from a single junction solar cell is established as 32% (Shockley & Queisser, 1961), which accounts for photon absorption, thermalization, and thermodynamic losses encountered in converting the electrochemical energy of electrons into free energy to perform work. However, given the additional charge separation step required in a DSSC, a realistic efficiency limit is likely to fall well below this Shockley-Queisser barrier due to restrictions on the allowable optical band gap (in order to maintain sufficient driving force for injection into TiO_2) and the significant loss of potential through the driving force required for regeneration of dye cations by the redox mediator.

If the semiconductor is chosen to be TiO_2 , which to date is the only material to produce efficiencies over 10%, then the absorption onset limit at which the injection yield can still remain close to unity is currently observed to be around 900 nm for a ruthenium triscyano terpyridyl complex (“black dye”) (Nazeeruddin, Pechy et al., 2001). Beyond this limit a larger proportion of the solar flux can be harvested, but the reduction in the lowest unoccupied molecular orbital (LUMO) energy of the dye lowers the free energy driving force for electron injection, causing a subsequent reduction in the injection yield. Assuming a 10% loss of incident photons due to reflection from the top glass surface of the anode, an idealized IPCE spectrum with an absorption onset of 900 nm can be created by presuming a rise to maximum IPCE over ~ 50 nm and light harvesting, injection and collection efficiencies of unity for all wavelengths between 400 nm and 850 nm (a situation which can already be achieved with sensitizers where the absorption onset is 750 nm and which has almost been achieved with the black dye itself). The maximum possible photocurrent can then be calculated by integrating the overlap of this IPCE spectrum with the AM 1.5 solar irradiance spectrum (Figure 3a), and yields a value of 30 mAcm^{-2} .

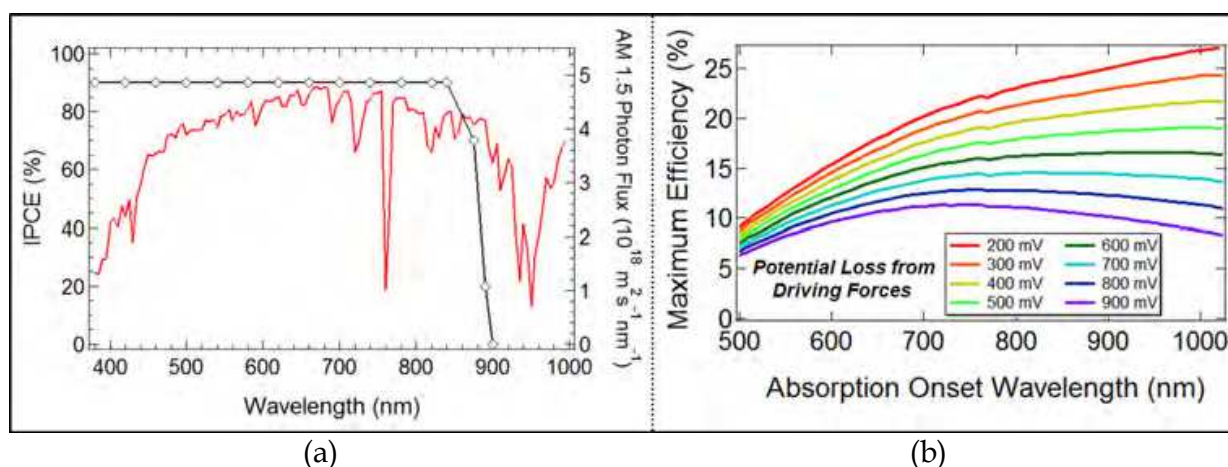


Fig. 3. (a) An idealized DSSC IPCE spectrum for a device with an absorption onset of 900 nm. The AM 1.5 solar irradiance spectrum (100 mWcm^{-2}) is also shown (red). (b) The maximum DSSC efficiency obtained from various absorption onsets with several possible potential energy losses from electron injection and dye regeneration driving forces.

To compute the maximum photovoltage, the free energy driving forces necessary to drive both electron injection and dye cation regeneration with yields of close to unity must be known. The sum of these driving forces is then removed from the optical band gap of the dye to calculate the maximum obtainable V_{oc} . There is a general lack of understanding regarding the minimum required driving forces, although previous studies indicate that the driving force required to achieve quantitative electron injection is ~ 200 mV (Hara, Sato et al., 2003; Katoh, Furube et al., 2002). The driving force required for dye regeneration will depend on the redox mediator, and is unusually high (~ 500 mV) for the commonly employed I^-/I_3^- system as this is a two electron process (Boschloo & Hagfeldt, 2009). If we assume that the regeneration driving force can be reduced to approximately 350 mV with an alternative redox mediator which involves only a single electron transfer, then the loss of potential from injection and regeneration driving force requirements would be 550 mV. Including the photon absorption, thermalization and energy conversion losses inside these driving force potentials, a 550 mV loss of potential would yield a maximum V_{oc} of 0.83 V.

Calculating the fill factor of a DSSC remains an ambiguous task. Bisquert et al. reported that the Shockley diode equation can be employed to calculate the fill factor as a function of the photovoltage. However, this approach requires knowledge of the diode ideality factor, which is still an unclear value for DSSCs (Bisquert & Mora-Sero, 2010). Since this is a matter of debate in the field, for the current calculations we have assumed a value of 0.70, which is either achieved or surpassed in many of the current benchmark devices. From equation (4), it is then possible to compute the maximum theoretical efficiency for such a DSSC. Since there will inevitably be debate about the acceptable assumptions for the maximum absorption onset and minimum driving forces for injection and regeneration, we have also computed the theoretical efficiency for several alternative values using a fill factor of 0.70 (Figure 3b). These values range from 14.5% (absorption onset 800 nm, loss of potential 700 mV) to 21.3% (absorption onset 950 nm, loss of potential 400 mV). Using realistic assumptions for absorption onset (900 nm) and loss of potential (550 mV), we calculate the maximum practical efficiency for a DSSC to be 17.6%. Considering the highest reported certified efficiency for a DSSC is 11.1%, there are clearly many limitations which still affect these devices and must be removed in order to approach this practical efficiency limit.

1.2 Porphyrin sensitizers in DSSCs

Emulation of the extraordinary chlorophyll-based photosynthetic light harvesting apparatus has inspired researchers to investigate synthetically prepared porphyrin dyes as sensitizers for dye-sensitized light harvesting applications (Kay & Grätzel, 1993), and they remain one of the most frequently studied dyes (Campbell, Burrell et al., 2004; Campbell, Jolley et al., 2007; Imahori, 2010). They are attractive for such purposes as their synthesis is relatively straightforward and their optical and electronic properties can be tuned via chemical modification of the porphyrin core (Dos Santos, Morandeira et al., 2010), the number of porphyrin units (Mozer, Griffith et al., 2009), and the linker between the core and the inorganic oxide (Lo, Hsu et al., 2010). It was originally assumed that porphyrin dyes would function identically to other analogous chromophores inside a DSSC, however, extensive studies of porphyrin dyes have shown that they are distinctive, and possess very different photophysics to the majority of other sensitizers (Bessho, Zakeeruddin et al., 2010; Campbell, Jolley et al., 2007; Imahori, Umeyama et al., 2009). The structure of some of these key porphyrin sensitizers are shown in Figure 4. Consequently, porphyrin dyes offer a unique opportunity to understand some fundamental limitations of DSSCs and trial innovative strategies which manipulate their unusual photophysical properties.

Porphyrin molecules typically display several strong visible light absorption bands due to the $\pi-\pi^*$ electron transitions of the macrocycle. Optical transitions from the two closely spaced highest occupied molecular orbitals (HOMO and HOMO + 1) to degenerate lowest unoccupied molecular orbitals (LUMOs) interact strongly to produce a high energy S_2 excited state with a large oscillator strength around 420 nm (Soret band), and a lower energy S_1 excited state with diminished oscillator strength between 500 nm and 650 nm (Q-band). Several Q-band absorptions are normally observed due to the vibronic transitions of the S_1 excited state, with the exact number depending on the symmetry of the porphyrin core (Gouterman, 1978). The position of these absorption bands can be tuned by structural modifications to the porphyrin molecule, and thus provide an extremely promising method of maximizing absorption of incident photon flux.

Porphyrin photoluminescence spectra display very small Stokes shifts and appear as two peaks due to transitions from different vibronic levels of the S_1 state back to the S_0 ground

state. Interestingly, metalloporphyrins, and in particular many zinc porphyrins, can display dual fluorescence, that is, emission from both the S_2 and S_1 excited states, due to the large energy gap between S_2 and S_1 excited states causing slow internal conversion. The relaxation dynamics of excited porphyrin complexes are well established. Singlet excited state lifetimes are normally ~ 1 ps from the S_2 state and ~ 2 ns from the S_1 state for metalloporphyrins and ~ 10 ns from S_1 for free base (metal free) molecules. Electrochemically porphyrin molecules are quite stable, with metalloporphyrins generally displaying two reversible oxidations of the porphyrin ring to form a radical cation or dication, while free base molecules generally show at least a single reversible oxidation. The assignment of the free base species is complicated by the stability of the mono and dications being strongly influenced by the identity of the solvent (Geng & Murray, 1986). The typical absorption, photoluminescence and electrochemical properties of porphyrin dyes are illustrated in Figure 5.

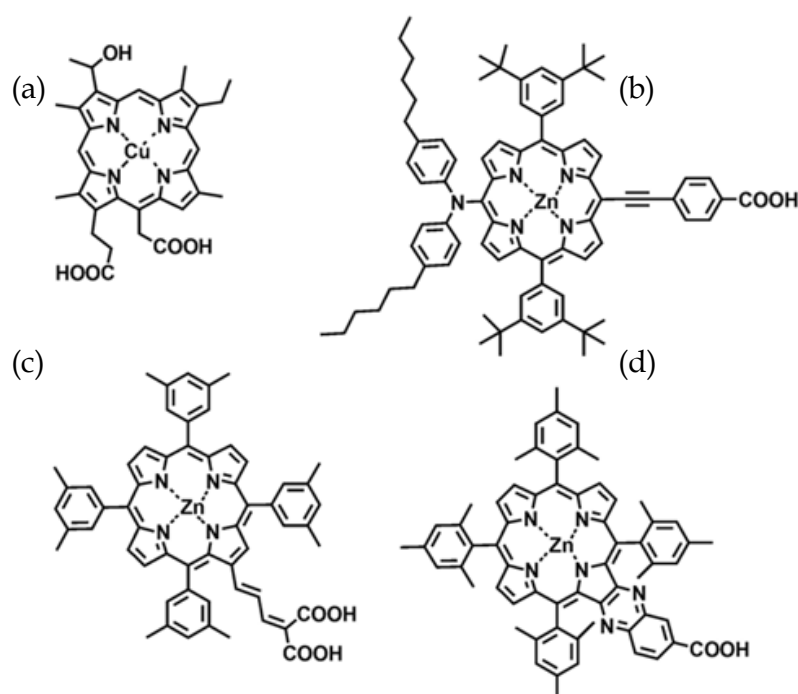


Fig. 4. The structure of (a) a pioneering synthetic porphyrin dye, and highly efficient porphyrin dyes (b) YD2, (c) GD2 and (d) Zn-4 published by various groups.

The development of new porphyrin dyes has been coupled with an increased understanding of the photophysics in operational DSSCs. For example, through various collaborations our group has previously shown that the luminescence lifetime, indicative of charge injection, depends on both the thermodynamic free energy driving force for injection and the conjugation through the linker moiety (Dos Santos, Morandeira et al., 2010). Furthermore, the electron lifetime in two of the most efficient porphyrin-sensitized solar cells was shown to be an order of magnitude lower than in identically prepared state of the art ruthenium bipyridyl (N719)-sensitized solar cells (Mozer, Wagner et al., 2008). This limitation can be somewhat circumvented by various post-treatments of the porphyrin-sensitized solar cells (Allegrucci, Lewcenko et al., 2009; Wagner, Griffith et al., 2011). However, despite this advanced understanding, the power conversion efficiencies of the best porphyrin-sensitized solar cells remains around 11%, well short of the theoretical maximum calculated earlier. The remainder of this chapter will focus on the fundamental limitations of these devices and explore some strategies which have been implemented to circumvent these limitations.

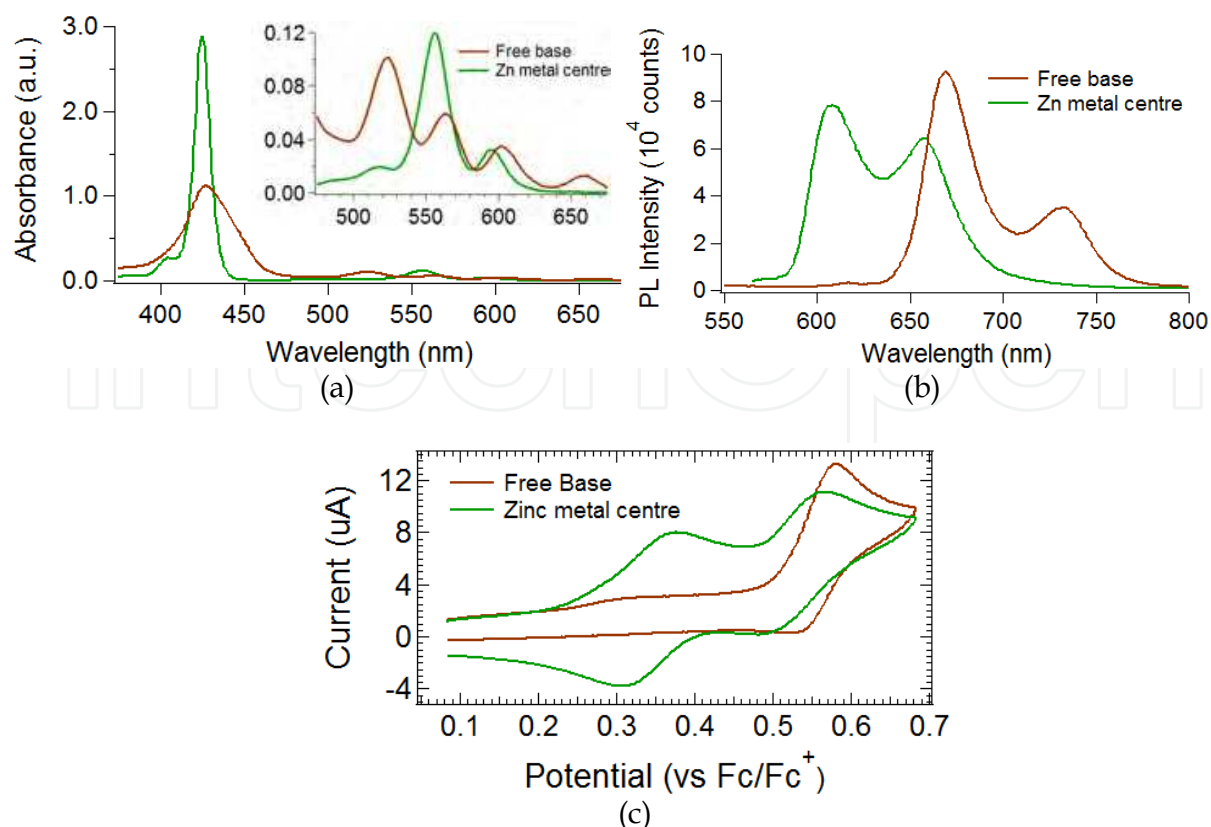


Fig. 5. The typical photophysical properties for 5×10^{-6} M solutions of zinc (green) and free base (brown) porphyrin molecules, showing (a) UV-vis absorption, (b) photoluminescence and (c) cyclic voltammograms (supporting electrolyte = 0.1 M TBAP).

2. Charge generation

The generation of free charges is the first critical step in achieving high efficiency in DSSCs. As indicated by equation (1), the charge generation processes consists of three steps; light absorption by the dye, injection of electrons from the photoexcited dye, and charge transport through the semiconductor film to prevent recombination. There are fundamental limitations with each of these three processes for porphyrin-sensitized solar cells. Some of these issues are intrinsic to the sensitizer and are difficult to remove. However, many of these basic problems can be circumvented using innovative approaches to device design. In this section we discuss some of the major limitations with charge generation in porphyrin-sensitized solar cells and summarize some of the important strategies that can be employed to reduce or indeed remove these limitations.

2.1 Light harvesting efficiency

Since the cross section for photon absorption of most photosensitizers is much smaller than the geometric area occupied on the semiconductor surface, light absorption by a pigment monolayer is small (Grätzel, 2005). To circumvent this, nanostructured semiconductor electrodes with a surface roughness factor (internal surface area normalized to the geometric area) on the order of a 1000 have been used, however these still require semiconductor films of at least $6 \mu\text{m}$ to produce a light harvesting efficiency close to unity. The requirement for this semiconductor thickness places significant constraints on the design of the DSSC. One

limitation is that dyes which are prone to recombination, such as porphyrin sensitizers, suffer increasing limitations with thicker semiconductor films due to the larger surface area for interfacial electron transfer reactions such as recombination. Furthermore, the viscosity of the electrolyte must be kept low to enable complete filling of the nanopores throughout the entire film thickness. Since such solvents are typically organic, their volatility leads to problems with hermetic sealing and long term stability of devices.

Incorporating multichromophore light harvesting arrays with increased absorption cross sections could potentially solve both of these issues, enabling efficient DSSCs with thinner films using ionic liquid (Kuang, Ito et al., 2006) or solid state electrolytes (Bach, Lupo et al., 1998). Multichromophore dyes could also allow novel electrode structures with smaller internal surface areas, such as nanotubes (Mor, Shankar et al., 2006), nanowires (Martinson, Elam et al., 2007), or large porosity mesoscopic structures to be employed. Our group investigated such an approach by joining two identical porphyrin chromophores together to create a dimer with twice the extinction coefficient but an unchanged molecular footprint on the semiconductor surface (Figure 6a). However, to ensure the enhanced light harvesting results in increased charge generation, efficient electron injection from both chromophores must be achieved. This condition is extremely difficult to demonstrate for dyes employing identical chromophores due to the matching spectroscopic features of each unit making them impossible to distinguish. In collaboration with Japanese co-workers we were able to produce the first spectroscopic evidence for electron injection from both chromophores of this porphyrin dimer by employing femtosecond time-resolved transient absorption (Mozer, Griffith et al., 2009). Since photons at the probe beam wavelength of 3440 nm are primarily absorbed by electrons in the TiO₂ in the absence of dye aggregates (Furube, Katoh et al., 2005), electron injection from the photoexcited dye is directly monitored by this technique. Furthermore, after normalization of the signal to correct for the absorbed pump beam intensity, a comparison of both the injection yield and kinetics can be performed. With reference to an N719 standard dye reference to determine the 100% injection yield value, the injection yield of the porphyrin dimer was determined to be ~70% (Figure 6b). The >50% quantum yield for the porphyrin dimer clearly demonstrates electron injection from *both* photoexcited porphyrin units within the dimer.

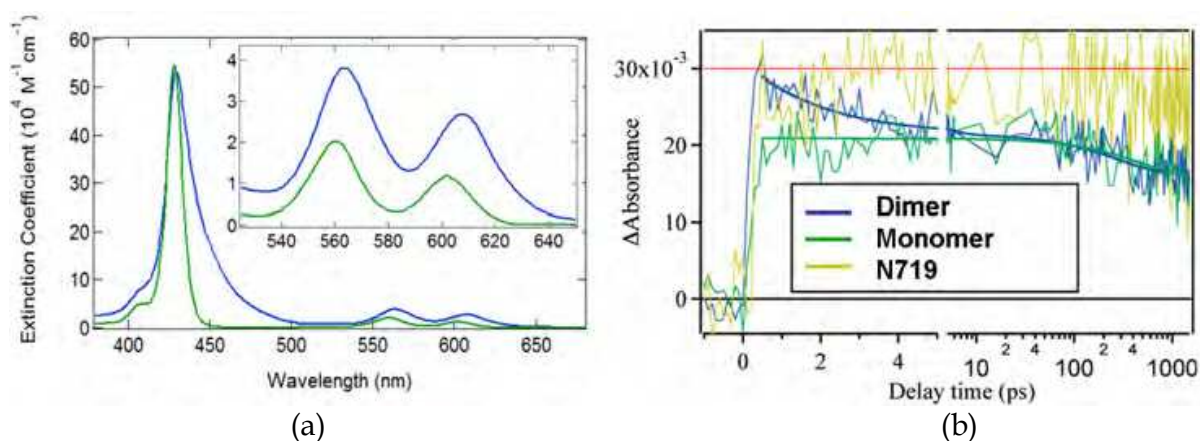


Fig. 6. Molar extinction coefficients of a porphyrin monomer (green) and dimer (blue) in solution. (b) Fs-TA signals (corrected for the absorbed pump intensity) of porphyrin-sensitized TiO₂ films in a redox containing electrolyte. An N719 signal obtained in air is also shown. Samples were excited by 150 fs pulses at 532 nm. Figure 6b taken from (Mozer, Griffith et al., 2009) and reproduced by permission of The American Chemical Society.

A second issue with light harvesting using porphyrin molecules is that the absorption bands of the sensitizers are quite discrete. Whilst the extinction coefficients in these absorption bands can be very high by employing for instance, a multichromophore dye, there are significant areas of the solar irradiance spectrum that are not covered by the absorption spectrum. Most notably, the vast majority of porphyrins do not absorb light beyond 700 nm. Additionally, the region between the Soret and Q-bands (450 nm-550 nm) also has a low absorption of incident photons. This lack of absorption significantly constrains the photocurrent which can be obtained from a porphyrin-based DSSC. Several strategies have been explored in an attempt to harvest an additional proportion of the incident solar flux using porphyrin dyes. One approach is to explore synthetic routes to extend the sensitizer absorption further towards the red end of the spectrum. Extension of the π conjugation and removal of symmetry in the porphyrin core can lead to splitting of the π and π^* levels and a decrease in the HOMO-LUMO gap, resulting in significant broadening and a red shift of the absorption bands. Imahori et al. were able to employ such an approach by using π -extended and fused porphyrin dyes to enhance the IPCE and overall device efficiency in a series of porphyrin molecules (Imahori, Umeyama et al., 2009).

A second approach used to extend the light harvesting efficiency of porphyrin-sensitized solar cells is to co-sensitize the semiconductor electrode with additional dyes which have complimentary absorption spectra to the porphyrin (Figure 7).

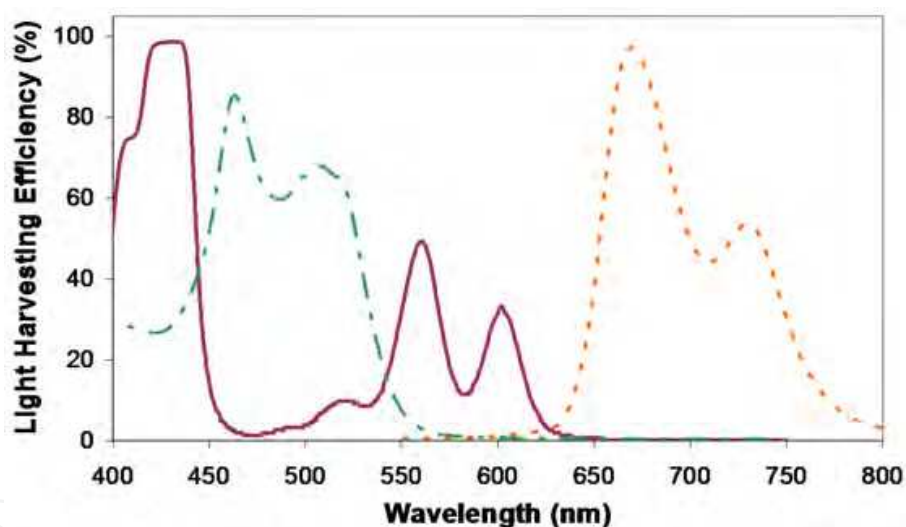


Fig. 7. An example of the extension in the porphyrin light harvesting efficiency (purple) that can be achieved by adding rhodium complex (green) and phthalocyanine (orange) dyes.

This approach has been utilized for many types of dyes, and was recently employed by Bessho et al. to enhance the photocurrent extracted from DSSCs prepared with a zinc porphyrin dye (Bessho, Zakeeruddin et al., 2010). The co-sensitization approach allows the absorption spectrum to be successfully extended; however, given the finite number of dye binding sites available on the semiconductor surface, there is still an intrinsic limitation on overall light harvesting potential. Our group explored methods to circumvent such limits by investigating a model system which combined free base and zinc porphyrin dyes. This study utilized not only the complimentary absorption spectra of the two dyes but also examined other possible synergistic interactions between the two dyes which are necessary in order to overcome the limit of a fixed amount of dye binding sites on the surface. We

were able to demonstrate an enhancement in both light harvesting *and* the injection yield when zinc and free base porphyrin dyes were combined on the same TiO₂ surface (Griffith, Mozer et al., 2011). Other groups have also pursued similar studies, focusing on extending the co-sensitization concept using energy relay systems. This approach involves dissolving the co-sensitizer in the electrolyte so that it no longer competes with the major sensitizer for binding sites on the semiconductor. Absorbed photon energy is transferred from the dissolved co-sensitizer to the chemically bound major sensitizer where it is then injected into the semiconductor. This approach achieved photocurrent enhancements of ~30% compared to direct co-sensitization on the same semiconductor surface (Hardin, Hoke et al., 2009).

2.2 Electron injection into semiconducting oxides

Electron injection from the photoexcited dye into the acceptor states of the semiconductor conduction band is perhaps the key mechanistic step in achieving efficient charge generation in DSSCs. According to the classical theory of electron transfer developed by Marcus, the rate of electron transfer, k_{ET} , between discrete donor and acceptor levels under non-adiabatic conditions is given by (Marcus, 1964):

$$k_{ET} = \frac{2\pi}{\hbar} \frac{H^2}{\sqrt{4\pi\lambda k_B T}} \exp\left(\frac{-(\lambda + \Delta G_0)^2}{4\pi\lambda k_B T}\right) \quad (5)$$

where H^2 is the electronic coupling between donor and acceptor states, ΔG_0 is the free energy driving force for electron transfer, λ is the total reorganization energy, T is the absolute temperature and \hbar and k_B the Planck and Boltzmann constants respectively. The electronic coupling (H^2) decreases exponentially with increasing distance, d , between the donor and the acceptor as:

$$H^2 = H_0^2 \exp(-\beta d) \quad (6)$$

where β is related to the properties of the medium between donor and acceptor, and H_0^2 is the coupling at distance $d = 0$. To achieve high efficiencies for injection in DSSCs, electron injection must be at least an order of magnitude faster than the competing deactivation of the dye excited state. Extensive studies of this charge separation process have typically shown sub-ps injection dynamics, suggesting electron injection competes efficiently with excited state decay, which occurs on the 1-10 ns timescale for porphyrin dyes. However, despite such fast kinetics, many porphyrin dyes still show very poor injection efficiencies. One possible reason for this poor injection is the heterogeneous nature of the process. Koops and Durrant demonstrated a distribution of injection half-life time constants from 0.1 – 3 ns for devices sensitized with various ruthenium polypyridyl dyes. They attributed this result to variations in the local density of acceptor states in the semiconductor for electron injection and therefore in the integrated electronic coupling, H^2 , for this reaction (Koops & Durrant, 2008). Since such behaviour is dependent on the density of states in the semiconductor and not on the dye itself, it would seem acceptable to assume that such heterogeneous injection kinetics also apply to porphyrin dyes, and thus there may be some slow injecting dyes which cannot compete with excited state deactivation.

The structure of the dye is clearly one crucial factor which will determine the injection efficiency. Campbell et al. investigated a wide range of porphyrin dyes and discovered that

the binding group which provides the electronic linkage between the chromophore and the semiconducting oxide plays an important role on the extracted photocurrent of devices. Given the similarity in the overall dye structures tested, this difference was attributed to variations in the injection efficiency achieved by varying the electronic coupling with different binding groups. Furthermore, the position of the binding group with respect to the porphyrin ring also affected the injection efficiency, with β -pyrrolic linked groups showing better efficiency than meso linked groups. Our group extended such investigations in collaboration with co-workers in England. It was shown using luminescence quenching coupled with time correlated single photon counting detection to probe injection, that both the conjugation in the linker moiety and the metallation of the porphyrin can affect the injection yield in porphyrin systems (Figure 8). Peripheral substituents in the meso positions of the porphyrin core have also been shown to effect injection, with bulky groups (phenyl or tert-butyl) providing steric hindrance effects which reduces dye aggregation or electron donating groups affecting the HOMO-LUMO gap of the dye and thus the driving force for injection (Lee, Lu et al., 2009).

	FbNC ^a	FbC ^a	ZnNC ^a	ZnC ^a	ZnC ^b
τ_{Zr} / ns	7.5	4.2	1.5	1.5	0.8
τ_{Ti} / ns	4.8	2.5	0.8	<0.1	0.6
$(k_{inj})^{-1}$ / ns	14	6.2	1.9	<0.1	1.7
J_{SC} / mAcm ⁻²	0.11	0.6	1.2	4.3	4.3

^a Kinetics for films covered with propylene carbonate. ^b Films covered with electrolyte.

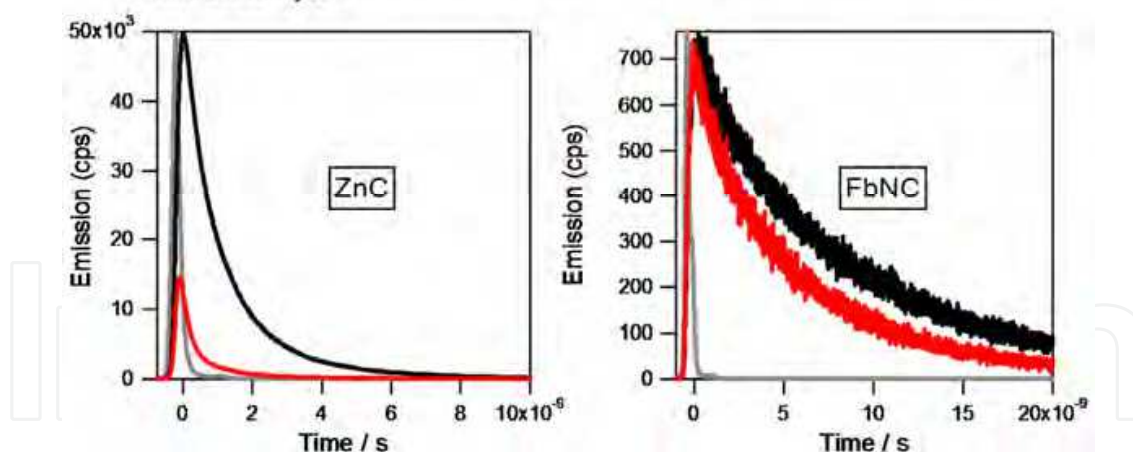


Fig. 8. (Top) Emission decay lifetimes, injection rate constants and device photocurrents for a series of porphyrin dyes with different metallation and linker conjugations. (Bottom) Transient emission decays of (a) a zinc porphyrin with a conjugated linker, and (b) a free base porphyrin with a saturated benzoic acid linker. Both dyes are adsorbed to TiO₂ (red), and ZrO₂, a high band gap semiconducting oxide which prevents electron injection (black). The instrument response function (IRF) is shown in grey. Figure taken from (Dos Santos, Morandeira et al., 2010) and reproduced by permission of The American Chemical Society.

Another concept which has been applied to improve injection in DSSCs is to synthesize dyes with an electron acceptor component close to the TiO₂ and an electron donor component

furthest from the TiO₂ linker. This ensures the electron density in the excited state is concentrated in the vicinity of the TiO₂, promoting injection and localizing the resultant positive charge away from the interface, thereby reducing recombination. Given the ease with which porphyrin compounds can be synthetically modified, this class of dyes offers an ideal system to explore this donor-acceptor concept. Clifford et al tested the theory by modifying a zinc porphyrin with a triphenylamine electron donor, and showed that recombination of the injected electron with the dye was an order of magnitude slower than for a comparable dye that lacked the electron-donor groups (Clifford, Yahioğlu et al., 2002). Hsieh et al extended such investigations when they tested a comprehensive range of electron donors and acceptors attached to the same porphyrin core. They demonstrated that several different electron donors attached to the optimal position of the porphyrin core were able to increase both the J_{sc} and the V_{oc} of the DSSCs, attributing this result to improved electron injection and reduced recombination due to the localization of electron density in the dye upon photoexcitation (Hsieh, Lu et al., 2010).

From equation (6) it is clear that the electronic coupling, and thus the rate of electron transfer for injection, is strongly dependent on the distance over which electron transfer occurs. If transfer between the porphyrin core and semiconductor occurs through the connecting binding group, extending the length of this group should reduce the speed with which injection occurs. Imahori et al tested this concept in a range of zinc porphyrin dyes, and found that contrary to expectation, the electron transfer process for longer linking groups were accelerated. They rationalized this result by postulating that some fraction of the porphyrin molecules are bound at an angle to the semiconductor surface as the linker becomes longer, with electron transfer in these dyes occurring through space, without facilitation through the linker. According to classical tunnelling theory, without the enhanced electronic coupling provided by the linker group, through-space injection could only occur if the sensitizer is within ~1 nm of the semiconductor surface. A distribution of electronic couplings from different injection routes would help explain the observed heterogeneity of the injection rates in DSSCs, however, dye orientation information remains quite limited. This lack of knowledge is problematic since the surface orientation of dyes will strongly affect the functioning of DSSCs, altering the effective barrier width for through-space charge tunnelling (Hengerer, Kavan et al., 2000) or the alignment of the dipole moment of the dye (Liu, Tang et al., 1996), which in turn can influence injection and recombination (Figure 9a). Several measurement techniques have been trialled, such as near edge X-ray absorption fine structure measurements (Guo, Cocks et al., 1997), scanning electron microscopy (Imahori, 2010), and X-ray photoelectron spectroscopy (Westermarck, Rensmo et al., 2002), however each of these techniques suffers from the requirement for high vacuum. Our group recently investigated employing X-ray reflectivity under ambient conditions to convert the measured interference spectra (Figure 9b) into a dye thickness and subsequently a molecular orientation for a dye/TiO₂ bilayer (Wagner, Griffith et al., 2011). However, this technique is still limited by the need for a flat surface rather than measuring nanoporous DSSC electrodes directly. Despite experimental difficulties with confirming orientation, the design of porphyrin dyes which can inject both directly through space or facilitated by the linker group presents a promising method for enhancing overall injection. In addition to modifying the dye structure to enhance injection efficiency, there are a range of additives which can be introduced to the electrolyte or sensitizing dye bath solutions to achieve enhanced injection. For instance, one potential issue with injection in porphyrin-sensitized solar cells is the limited free energy driving forces available for some dyes. This

becomes a problem for dyes with a large red-shift in the standard porphyrin absorption spectrum, and in particular, the free base porphyrin dyes, which can often display LUMO energies approaching that of the semiconductor conduction band potential. The absence of significant free energy driving forces is intrinsic to the dye/semiconductor combination, and is difficult to alter with structural modifications of the dye. However, the conduction band edge potential (E_{CB}) is related to the surface potential of the oxide. Introducing charged species into the electrolyte which subsequently adsorb to the semiconductor surface can therefore shift the value of E_{CB} and change the relative driving force for injection. Placing alkali metal cations in the electrolyte is the most common way to achieve a positive shift of E_{CB} , thereby improving the injection driving force for dyes with low (more positive) LUMO energies (Liu, Hagfeldt et al., 1998). Another additive which has been shown to improve injection in porphyrin-sensitized solar cells is chenodeoxycholic acid (CDCA). This additive is generally dissolved in the sensitizing dye solution and acts to prevent aggregation of the dyes on the surface, a significant issue for porphyrin sensitizers, which interact strongly through π - π stacking forces (Planells, Forneli et al., 2008). Surface aggregation induces injection from excited dyes into neighbouring dye molecules, thus reducing the injection efficiency through a self-quenching mechanism. CDCA molecules co-adsorb to the oxide surface with the dye, preventing aggregate formation and elevating the injection efficiency.

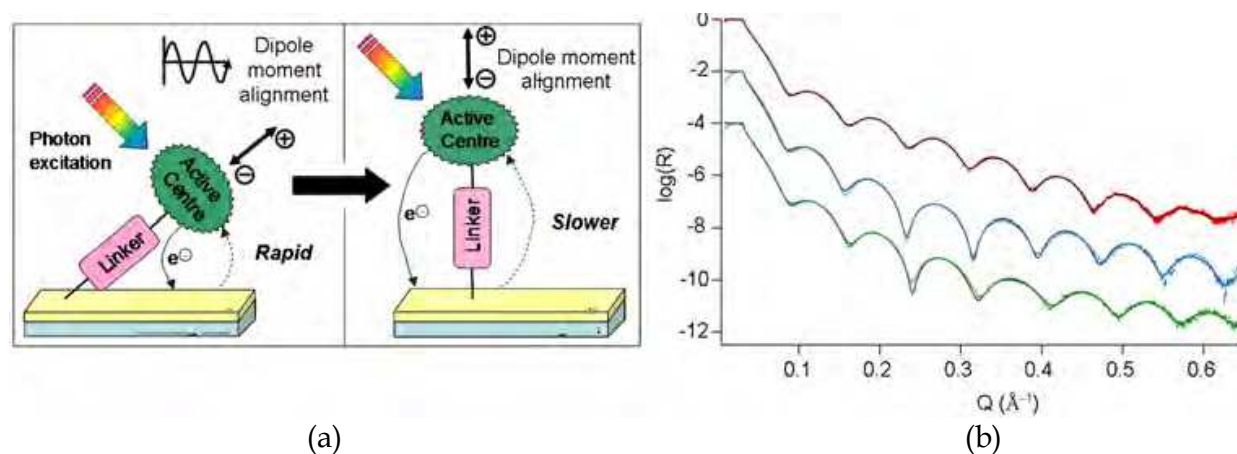


Fig. 9. (a) An illustration of the effect of dye adsorption orientation on the charge transfer and dipole alignment at a dye sensitised electrode. (b) Observed (data points) and calculated (solid lines) X-ray reflectivity spectra for a TiO_2 substrate (red), and porphyrin-sensitized TiO_2 before (blue) and after (green) 1 hour light exposure. Figure 9b taken from (Wagner, Griffith et al., 2011) and reproduced by permission of The American Chemical Society.

An alternative method to electrolyte additives which can be employed to modulate the semiconductor conduction band is to change the material employed as the semiconductor. The density of states (DOS) distribution for semiconductors is normally expressed as an exponential function with a characteristic broadening parameter, unique for each different metal oxide. As such, different materials will display various potentials at matched electron densities, leading to different E_{CB} values (Grätzel, 2001). In order to obtain a more positive E_{CB} to enhance the driving force for injection, the standard TiO_2 semiconductor can be replaced with materials such as SnO_2 (Fukai, Kondo et al., 2007), In_2O_3 (Mori & Asano, 2010) or WO_3 (Zheng, Tachibana et al., 2010), which all possess a narrower DOS distribution and thus lower E_{CB} values than TiO_2 at the same charge densities. Each of these materials

produce higher photocurrents than TiO₂-based systems due to enhanced injection, however the electron mobility in these oxides is much higher than in TiO₂ and thus they suffer from faster recombination reactions which minimize or can even reverse the overall efficiency gains achieved by enhancing injection.

The injection yield of porphyrin-sensitized devices can also be improved by innovative device design or the use of various post-treatments to improve the system. Our group recently explored such post-treatments, demonstrating improvements in the J_{sc} of a zinc porphyrin DSSC arising from enhanced injection after the cell was exposed to AM 1.5 illumination for 1 hr (Wagner, Griffith et al., 2011). The injection yield was measured using absorbed photon-to-current conversion efficiency (APCE), which is calculated by normalizing the IPCE for light absorption:

$$APCE = \frac{IPCE}{LHE} = \phi_{inj} \eta_{coll} \quad (7)$$

By employing thin ($\sim 2 \mu\text{m}$) film DSSCs, transport losses are assumed to be negligible and thus η_{coll} is close to 100% and the APCE measurements enable determination of ϕ_{inj} under short circuit conditions. The increased APCE (from 65% to approximately 90%) following light exposure (Figure 10a) therefore demonstrated an increased injection yield for the porphyrin dye. We have also employed APCE measurements to demonstrate an enhancement in the injection yield when zinc and free base porphyrin dyes were combined on the same TiO₂ surface. The APCE of the mixture was $\sim 300\%$ higher than either individual dye. It was proposed that this enhanced injection could arise from energy transfer from the zinc dye with an inefficient linker to the free base dye which possesses a conjugated linker, possible due to the spectral overlap between zinc porphyrin emissions and free base porphyrin absorption (Griffith, Mozer et al., 2011). This process could allow the zinc dye to inject through a more efficient conjugated pathway on the free base dye (Figure 10b).

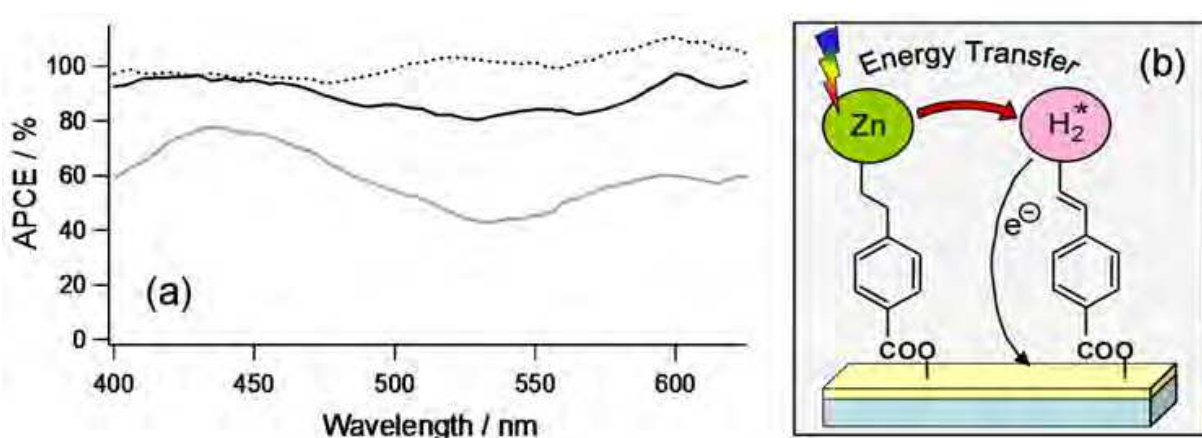


Fig. 10. (a) Absorbed photon to current conversion efficiencies (APCE) which estimate the injection yield for porphyrin-sensitized thin-film TiO₂ devices before (grey solid line) and after (black solid line) 1 hour light exposure. Data for the N719 dye is included for comparison (dashed line). (b) Energy transfer from a zinc to a free base porphyrin to utilize the conjugated injection pathway. Figure 10a taken from (Wagner, Griffith et al., 2011) and reproduced by permission of The American Chemical Society.

2.3 Charge transport

Since the nanoparticles of typical DSSC anodes are too small to sustain a space charge layer, electron transport in DSSCs is dominated by diffusion with negligible drift contributions. In this situation, the charge collection efficiency, η_{coll} , is related to the electron diffusion coefficient (D) and electron lifetime (τ) in the semiconductor electrode (where electron lifetime is the average time spent in the electrode). If the electron diffusion length, L , where:

$$L = \sqrt{D\tau} \tag{8}$$

is shorter than the thickness of the semiconductor electrode, then electrons will recombine with the dye cation or the acceptor species in the redox mediator during charge transport, limiting η_{coll} . Typical diffusion lengths for the benchmark ruthenium dyes are 30-60 μm , leading to high collection efficiencies on 20 μm semiconductor films. The diffusion coefficients for porphyrin DSSCs are comparable to most other dyes. However, many porphyrins, and in particular free base dyes, suffer from high levels of recombination which lower the electron lifetime and thus the diffusion length. The effective diffusion length of sensitizers can be estimated from the film thickness at which the measured IPCE or J_{sc} saturates. However, such measurements cannot deconvolute the competing affects of increasing light harvesting and decreasing collection efficiency. Since the film thickness required for unity absorption of incident photons is $\sim 6 \mu\text{m}$, J_{sc} saturation values below this limit suggest there will be charge transport losses, as has been measured for some porphyrin DSSCs (Figure 11a). To determine L , D and τ values more rigorously, small amplitude perturbation techniques such as intensity modulated photovoltage or photocurrent spectroscopy, impedance spectroscopy or stepped-light induced measurements of photocurrent and photovoltage are generally employed, producing plots such as the one displayed in Figure 11b. However, there is some debate regarding the accuracy of these transient techniques, with Barnes et al. arguing that IPCE measurements performed with front and backside illumination are more relevant than small perturbation relaxation techniques (Barnes, Liu et al., 2009). In order to remove or minimize the charge transport losses in some porphyrins, strategies which reduce the recombination must be explored.

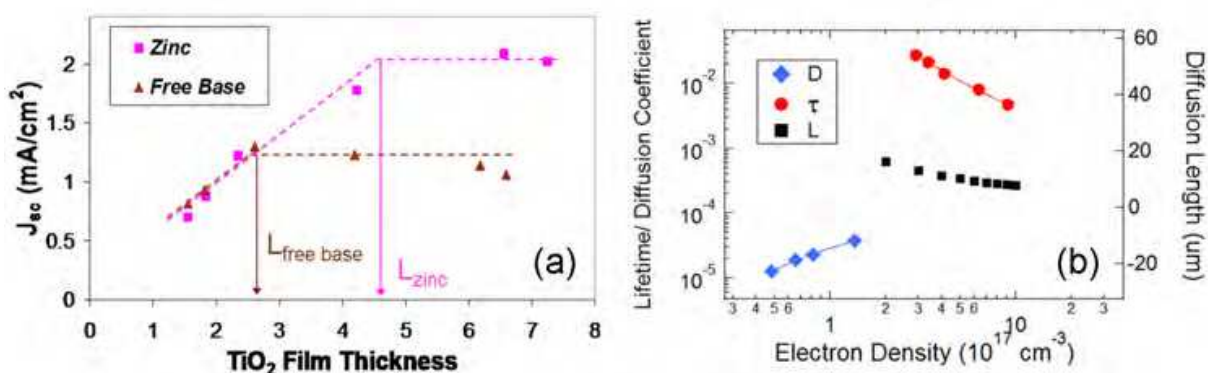


Fig. 11. (a) Diffusion length estimated from J_{sc} saturation values for inefficient zinc and free base porphyrins. (b) D (blue diamonds) and τ (red circles) values measured by stepped light-induced photovoltage and photocurrent techniques plotted against electron density for a porphyrin-sensitized DSSC. The calculated electron diffusion length, L , is also shown (black squares).

3. Charge recombination

As described earlier, the J_{sc} of porphyrin-sensitized solar cells is determined by their spectral response, injection efficiency and charge transport characteristics, all of which are quite well understood. Conversely, the open circuit voltage (V_{oc}) of porphyrin DSSCs is generally observed to be 100–200 mV lower than the commonly used ruthenium dyes, the origin of which is only partially elucidated. Since the photovoltage under illumination is dependent on the Fermi level in the semiconducting oxide, the lower V_{oc} for porphyrin DSSCs may be related to either a positive shift of the conduction band potential (E_{CB}) of the semiconducting oxide following dye sensitization or a lower electron density due to a reduced electron lifetime. Our group investigated each of these possibilities in collaboration with Japanese co-workers in order to determine the origin of the lower V_{oc} in porphyrin DSSCs. It was found that when the V_{oc} was plotted against the electron density (ED) in the TiO_2 film, neither the slope nor the y-intercept of the V_{oc} vs logED plot differed between ruthenium and porphyrin sensitized solar cells (Mozer, Wagner et al., 2008) (Figure 12d). Since the redox mediator Fermi level was constant in each case, the V_{oc} vs logED plot is indicative of the TiO_2 conduction band potential. Hence these results demonstrated that the lower V_{oc} of porphyrin-sensitized solar cells is not due to an E_{CB} shift following dye uptake. We found instead that the low photovoltages were a result of electron lifetimes in porphyrin dyes being reduced by a factor of ~ 200 at matched electron densities, independent of their chemical structure (Figure 12b). Furthermore, we showed that the shorter electron lifetimes were not related to electron transport differences, since the diffusion coefficients were identical for porphyrin and ruthenium dyes (Figure 12c).

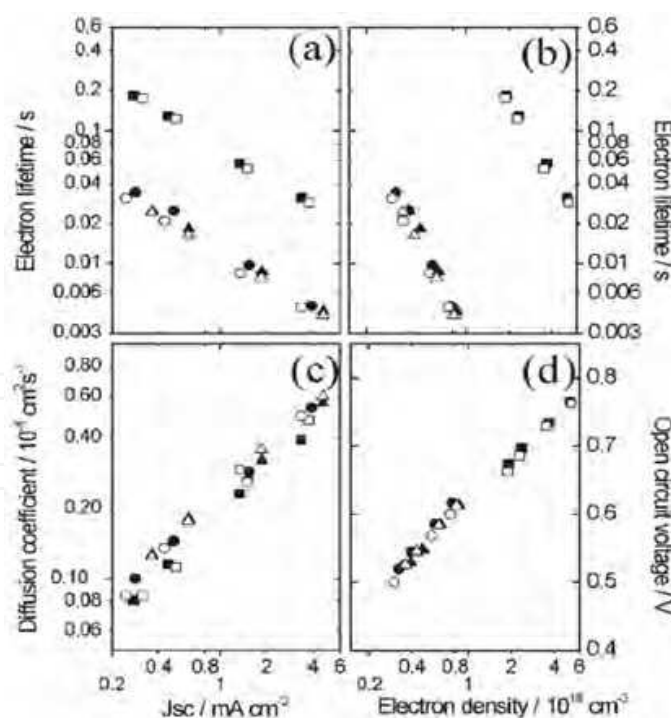


Fig. 12. (a) Electron lifetime and (c) diffusion coefficient versus short circuit current density. (b) Electron lifetime and (d) open circuit voltage versus electron density for ruthenium (squares) and porphyrin (circles, triangles) DSSCs. Figure taken from (Mozer, Wagner et al., 2008) and reproduced by permission of The Royal Society of Chemistry

Since charge is a conserved quantity in any system, a continuity equation for the charge density, n , can be derived for a DSSC. The time-dependent form of this equation is:

$$\frac{\partial n}{\partial t} = \phi_{inj} \alpha I_0 \exp(-\alpha x) + D_0 \frac{\partial^2 n}{\partial x^2} - \left(\frac{n}{\tau_{redox}} + \frac{n}{\tau_{dye}} \right) \quad (9)$$

where the first term on the right-hand side of the equation describes the electron injection into the oxide from dyes at position x (α is the absorption coefficient, I_0 is the incident photon flux and $x = 0$ at the anodic contact). The second term accounts for the diffusion of electrons (D_0 is the diffusion coefficient of electrons), whilst the third term describes the two simultaneously occurring recombination reactions (where τ_{redox} and τ_{dye} are the lifetimes determined by the recombination reactions of conduction band electrons with the redox acceptor species and the oxidised dye, respectively). Since the lower V_{oc} of porphyrin DSSCs arises from a reduced electron lifetime which is not affected by electron transport, it must be related to an enhancement in one (or both) of the two recombination processes.

Dye cation recombination in DSSCs has been extensively studied using transient absorption spectroscopy to probe the rate of disappearance of the dye cation absorption following its creation. For the majority of dyes, the cations are regenerated with a time constant of 1-10 μ s, even in viscous or semi-solid electrolytes which slow down the reaction due to diffusion limitations (Nogueira & Paoli, 2001; Wang, Zakeeruddin et al., 2003). These kinetics are generally much faster than the recombination reaction between dye cations and electrons in the semiconductor, which has a time constant of 100 μ s – 1 ms (Willis, Olson et al., 2002). Our group has demonstrated this situation holds true for porphyrin dyes by measuring transient absorption kinetics for the dye cation (with an absorption peak at 700 nm) in the absence and the presence of a standard I⁻/I₃⁻ redox mediator (Figure 13). Without the redox mediator the half signal decay was 60 μ s, whilst in the presence of the redox mediator, the half-signal decay was accelerated to 2 μ s (Wagner, Griffith et al., 2011). This suggests efficient prevention of recombination through regeneration of the dye cations by the redox mediator. It is therefore very unlikely that the short electron lifetime for porphyrin DSSCs results from recombination with the dye cation.

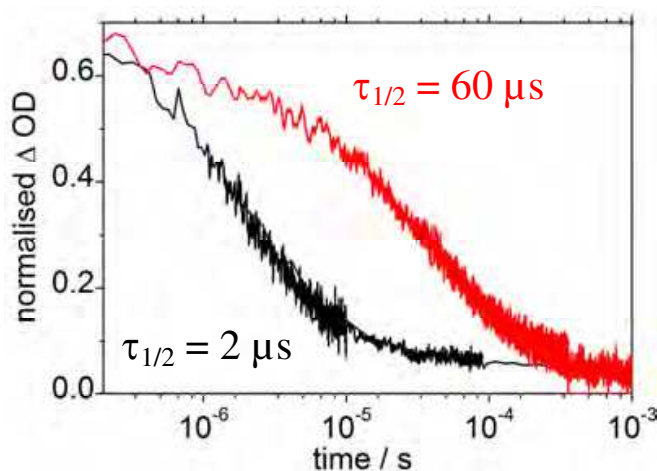


Fig. 13. Transient absorption kinetic traces recorded at 700 nm for porphyrin-sensitized TiO₂ films covered with acetonitrile electrolyte in the absence (red) and presence (black) of an I⁻/I₃⁻ redox mediator. The films were photoexcited by nanosecond pulses at 532 nm.

As dye cation recombination is a negligible problem for porphyrin DSSCs, the shorter electron lifetime must arise from increased recombination between conduction band electrons and the acceptor species in the redox mediator. Such a process can only occur from an increased proximity of the acceptor species to the semiconductor surface. For the standard I^-/I_3^- redox mediator, it has been proposed that most organic dyes (specifically including porphyrins) either attract I_3^- to the dye–semiconductor interface (Miyashita, Sunahara et al., 2008) or catalyse the recombination reaction with acceptor species in the electrolyte, such as I_3^- or the iodine radical I_2^- (O'Regan, López-Duarte et al., 2008). Several different strategies have been implemented in an attempt to improve the electron lifetime, and we now examine some of the major innovations which have led to enhancements in the overall device V_{oc} .

3.1 Molecular structure

The molecular structure of dyes can have a large impact on the concentration of the redox mediator at the semiconductor surface. Nakade et al. reported that adsorption of ruthenium dye N719 will decrease the concentration of acceptor species I_3^- in the vicinity of the TiO_2 surface due to shielding from the negative SCN^- ligands on the dye molecule (Nakade, Kanzaki et al., 2005). A similar physical shielding effect can be achieved with organic dyes by introducing bulky substituent groups to sterically hinder the approach of the redox mediator to the semiconductor surface (Koumura, Wang et al., 2006) (Figure 14). This approach was shown to increase the electron lifetime and V_{oc} for DSSCs constructed with carbazole (Miyashita, Sunahara et al., 2008), phthalocyanine (Mori, Nagata et al., 2010) and osmium (Sauvé, Cass et al., 2000) complexes. Several of these authors reported minimal effects when the dye loading on the surface was reduced, confirming that the structure of the dye, and its steric crowding of the semiconductor surface, was the major factor driving the increase in electron lifetime. This strategy has been successfully implemented to porphyrin sensitizers, with the introduction of octyl chains to a high efficiency zinc porphyrin dye producing the highest efficiency ionic liquid-based porphyrin DSSC (Armel, Pringle et al., 2010). Imahori et al. have demonstrated the value of amending the porphyrin structure by adding bulky mesityl groups at the meso positions of the porphyrin core to both reduce the dye aggregation (which limits electron injection) and enhance the V_{oc} by blocking the surface from the approach of the redox mediator.

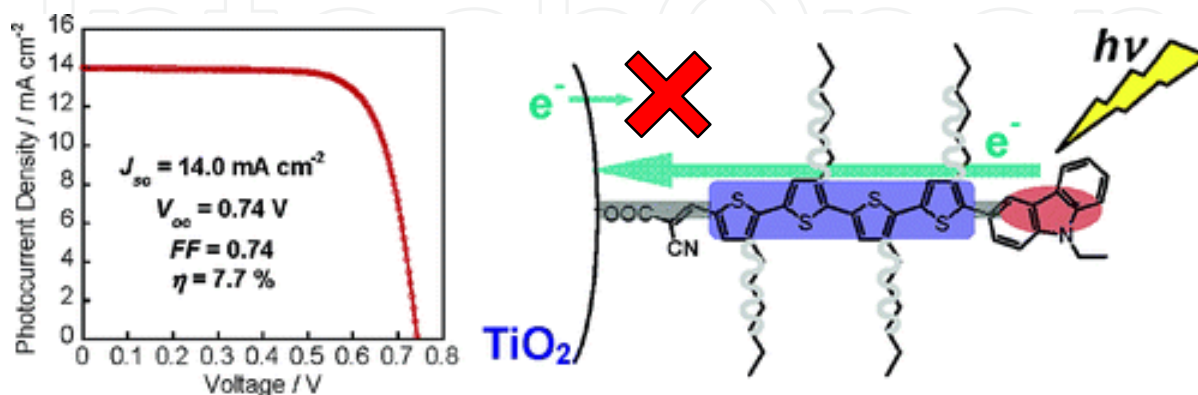


Fig. 14. PV parameters and an illustration of a carbazole dye with long alkyl chains to stop the redox mediator reaching the semiconductor surface. Figure taken from (Koumura, Wang et al., 2006) and reproduced by permission of The American Chemical Society.

3.2 Semiconductor blocking effects

As was earlier described for electron injection, strategies to inhibit recombination between conduction band electrons and the redox mediator can focus on either the dye or the semiconductor side of the major electronic interface. Accordingly, an alternative strategy to dye structure modification which can be employed to extend the electron lifetime in porphyrin DSSCs is to insulate exposed sites on the semiconductor surface. Rather than block the approach of the redox mediator to these active sites, this method attempts to deactivate the electron transfer process at these sites using an insulating surface covering. Deposition of a compact TiO₂ layer from a titanium tetrachloride (TiCl₄) precursor has been previously used to block electron transfer between the redox mediator and the back FTO-glass contact (Burke, Ito et al., 2008), and the same approach has also been successfully applied to insulating the semiconductor surface. O'Regan et al. utilized photocurrent and photovoltage transient measurements to show that deposition of a compact TiO₂ blocking layer on top of the mesoporous TiO₂ electrode produces an 80 mV downward shift in the TiO₂ conduction band edge potential and a 20-fold decrease in the electron/electrolyte recombination rate constant (O'Regan, Durrant et al., 2007). Following these findings, a range of organic acids have been trialled as surface insulating agents. Phosphinic acids are particularly useful in this regard since they form strong bonds with titania but, in contrast to commonly employed carboxylic or phosphonic acids, also have two organic substituents which can potentially provide more complete insulation of the semiconductor surface. Accordingly our group, in collaboration with Australian co-workers, employed a phosphinic acid surface treatment to a zinc porphyrin DSSC and demonstrated a successful suppression of the surface recombination and a simultaneous positive conduction band shift, resulting in 15% improvements in the photocurrent and 20% increases in the overall device efficiency. Measurements of time-resolved photovoltage transients demonstrated that these improvements resulted from an increased electron lifetime (Figure 15a), although the expected V_{oc} improvement was limited by a simultaneous positive shift in the semiconductor conduction band potential (Allegrucci, Lewcenko et al., 2009) (Figure 15b). Nonetheless, these results establish that the short electron lifetimes which limit porphyrin DSSCs can be improved with a semiconductor surface treatment.

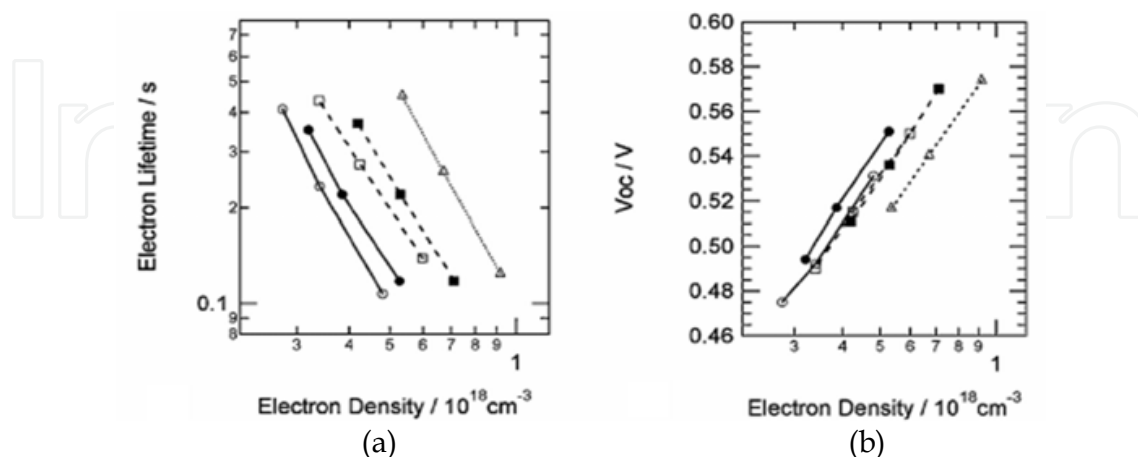


Fig. 15. (a) Electron lifetime, and (b) V_{oc} , as a function of electron density in the TiO₂ film for porphyrin DSSCs after 0 mins (circles), 5 mins (squares) and 30 mins (triangles) of a phosphinic acid surface treatment. Figure taken from (Allegrucci, Lewcenko et al., 2009) and reproduced by permission of The Royal Society of Chemistry.

3.3 Manipulating interfacial charges

The predominate recombination pathway in porphyrin DSSCs is between electrons and the acceptor species in the redox mediator. Consequently, the cations and additives which are typically dissolved in the electrolyte play an important role in mediating this reaction. The roles of the cations have been found to influence the electron injection yield, the open-circuit voltage, the electron diffusion coefficient, and the rate of dye-cation regeneration (Kambe, Nakade et al., 2002; Zaban, Ferrere et al., 1998). With careful design, the influence of these supporting cations can be manipulated to remove the acceptor species in the redox mediator from the vicinity of the semiconductor surface, thereby extending the electron lifetime and raising the V_{oc} . Nakade et al investigated such effects by varying the size of the cation additive for a ruthenium-sensitized solar cell with a standard I^-/I_3^- redox mediator. They found that the size of the cation has a large impact on the thickness of the electrical double layer (Helmholtz and diffuse layers), effectively altering the local (surface) concentration of I_3^- , which is the concentration of I_3^- within the distance from the TiO_2 surface at which electrons can be transferred (Nakade, Kanzaki et al., 2005). When electrons are injected into the TiO_2 , the surface becomes negatively charged and an electrical double layer is formed at the surface. For cations which are small enough to penetrate between the adsorbed dye molecules this double layer is formed over ~ 1 nm, effectively screening the surface charge and allowing I_3^- to approach close to the TiO_2 surface. However, for bulky cations such as tetrabutylammonium (TBA^+) which cannot penetrate between the dye and TiO_2 , a distance much longer than the size of the dye is needed for the screening. In this case, anions feel a repulsive force to penetrate between the dye and TiO_2 due to the negative surface charge. This reduces the local I_3^- concentration and results in a longer electron lifetime (Figure 16).

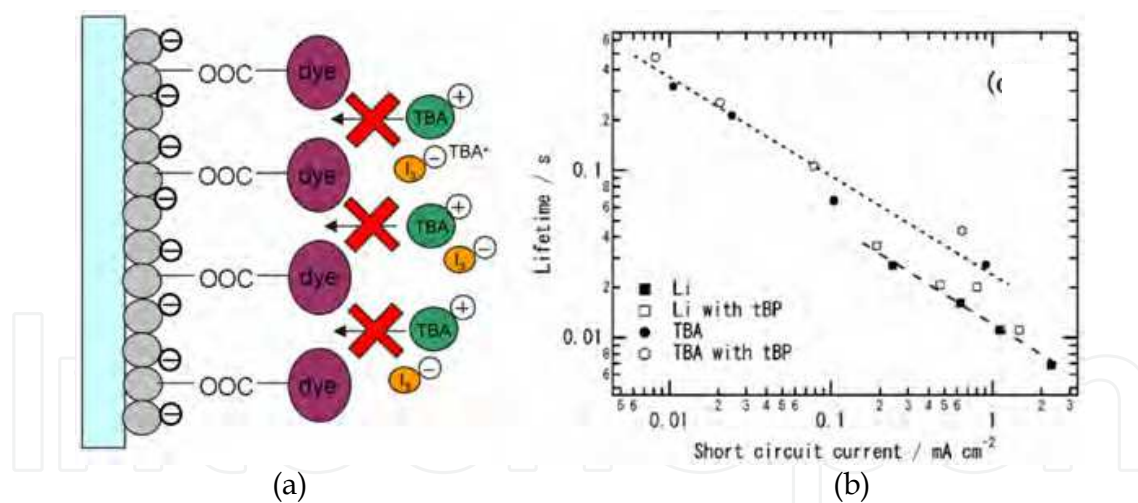


Fig. 16. (a) The extended electric double layer at the surface using a bulky supporting cation. (b) The electron lifetime for DSSCs employing TBA^+ and Li^+ in the electrolyte. Figure 16b taken from (Nakade, Kanzaki et al., 2005) and reproduced by permission of The American Chemical Society.

Nakade et al. showed that this increased electron lifetime led to a 300 mV increase in V_{oc} , although the increase was aided by a negative shift in E_{CB} which reduced the photocurrent. Since such an approach simply manipulates the position of intrinsically formed charged layers using a generic electrolyte, it should be generally applicable to all dye systems, including porphyrins.

Post-treatments or dye interactions could also lead to longer electron lifetimes and improved V_{oc} in porphyrin DSSCs. Our group have demonstrated using photovoltage decay measurements that exposure of a zinc porphyrin DSSC to AM 1.5 illumination conditions for a period of 1 hour produces an increase in the electron lifetime by a factor of 2 to 3. This result was also accompanied by a comparable decrease in the electron diffusion coefficient. The improved electron lifetime combined with the increased J_{sc} obtained from the same post-treatment resulted in increased electron densities at open circuit conditions, leading to improved V_{oc} (Wagner, Griffith et al., 2011). It was postulated that the origin of this effect could be either the photo-generation of electronic states within the band gap of TiO_2 or a change in the behavior of electrolyte additives when the solar cell is illuminated, both of which could lead to improved injection, longer electron lifetimes and slower electron transport.

Charge transfer interactions could also act to decrease recombination in porphyrin DSSCs in certain circumstances. Our group recently reported an enhanced injection yield when zinc and free base porphyrin dyes were combined, however we also noted that this mixture resulted in a higher V_{oc} than that obtained from both individual dyes. Measured energy levels for the two dyes indicate that the zinc dye (ZnNC) had both a higher HOMO and a higher LUMO energy than the free base dye (FbC), which could lead to hole transfer from FbC^+ to neutral ZnNC (Figure 17a). It was noted that similar charge transfer processes between zinc and free base porphyrins have been previously observed to occur on very fast (picosecond) timescales (Koehorst, Boschloo et al., 2000). It was speculated that hole transfer (HT) could potentially improve the charge generation yield of FbC by preventing recombination. This would be feasible if $k_{HT} \gg k_{EDR,FbC} \gg k_{DR,FbC}$, where $k_{EDR,FbC}$ is the rate constant for charge recombination between TiO_2 electrons and FbC^+ , and $k_{DR,FbC}$ is the rate constant for dye regeneration of FbC (Griffith, Mozer et al., 2011) (Figure 17b). Such charge transfer processes have been shown to reduce recombination and improve the V_{oc} for other co-sensitized DSSC systems (Clifford, Forneli et al., 2011; Clifford, Palomares et al., 2004), and offer an attractive pathway to simultaneously remove both injection and recombination limitations in porphyrin DSSCs.

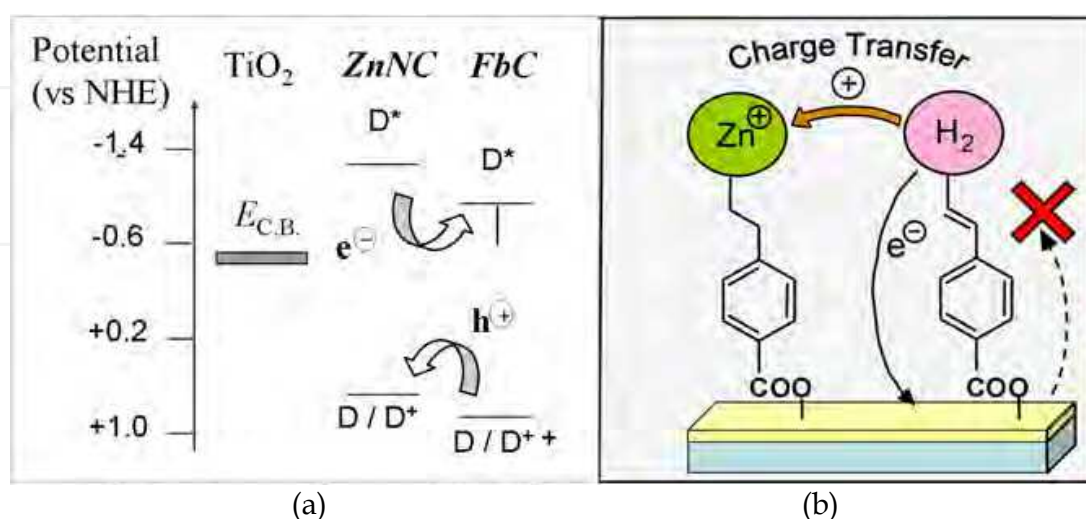


Fig. 17. (a) Calculated dye HOMO and LUMO energy levels and potential charge transfer processes for a zinc/free base mixed dye system. (b) Charge transfer from oxidized free base to neutral zinc molecules to prevent recombination.

4. Conclusion

The efficient light harvesting potential of porphyrin dyes, exemplified by their primary role in photosynthesis, makes them ideal candidates for use as photosensitizers within dye sensitized solar cells. Their synthesis is relatively straightforward, and their optical and electronic properties can be tuned via chemical modification of the coordinating metal centre, the porphyrin core, the number of porphyrin units, and the linker between the core and the inorganic oxide. Recent porphyrin DSSC developments have been accompanied by a simultaneous improvement in the understanding of the photophysics governing operational solar cells. In particular, many of the fundamental limitations which constrain the performance of these dyes have been elucidated.

The major limitations which continue to hinder the performance of porphyrin DSSCs are the light harvesting of incident photons, injection into the semiconducting oxide and the recombination with the acceptor species in the redox mediator. Light harvesting limitations, which mainly surround the limited absorption of low energy (red) photons, can be circumvented by combining several dyes with complimentary absorption spectra or by employing multichromophore dyes to boost the effective absorption coefficients and allow thinner semiconductor films to be employed. Electron injection yields for porphyrin dyes, studied by techniques including time resolved luminescence quenching, ultrafast transient absorption spectroscopy and absorbed photon-to-current conversion efficiency, have been shown to be much lower than the kinetics of injection compared to dye deactivation would predict. Such limitations can be caused by dye structural considerations, heterogeneous injection kinetics, or poor free energy driving forces. These limitations can be addressed by modifying the dye structure, addition of various chemicals to the electrolyte to modify the free energy driving force for injection, employing post-treatments to enhance injection efficiency after fabrication or by combining different dyes to achieve improved injection efficiencies through synergistic interactions. Recombination limitations, now understood to be the major impediment to achieving high efficiency in porphyrin DSSCs, have been shown to arise from the back reaction between electrons in the oxide conduction band and the acceptor species in the redox mediator. Characterization of the electron lifetime, studied by techniques such as intensity modulated voltage spectroscopy (IMVS), electrochemical impedance spectroscopy and stepped-light induced measurements of photocurrent and photovoltage (SLIM-PCV) reveals that this recombination reaction can be influenced by several factors, such as a physical blocking effect on either the dye structure or the semiconductor surface, electrostatic interactions which control the location of charges at the interface or combining dyes to harness various photoinduced charge transfer mechanisms.

Given the attractive features of porphyrin chromophores, the improved understanding of porphyrin DSSCs which has been compiled in recent years, and the many innovative strategies still emerging, there remains much promise in the development of these devices. Porphyrin based DSSCs continue to offer a fruitful topic for exploring the fundamental processes which limit the efficiency of dye-sensitized light harvesting applications, inspiring the development of innovative strategies to circumvent these basic limitations. The remaining challenge is to integrate each of these new strategies to produce a porphyrin DSSC with a power conversion efficiency which surpasses the current maximum of 11% and allows these devices to become a commercial reality.

5. Acknowledgments

The authors gratefully acknowledge the financial support of the Australian Research Council through the ARC Centre of Excellence Federation Fellowship, Discovery, and LIEF schemes. MJG acknowledges the additional support of an Australian Postgraduate Award and a Prime Minister's Asia Australia Endeavour Award from the Australian Federal government. The authors would like to thank, in no particular order, Prof. David Officer, Prof. Gordon Wallace, Dr Kaludia Wagner, Dr Pawel Wagner, Prof. Keith Gordon, Dr Ryuzi Katoh, Assoc. Prof. Akihiro Furube and Assoc. Prof. Shogo Mori for their invaluable collaborations and fruitful discussions.

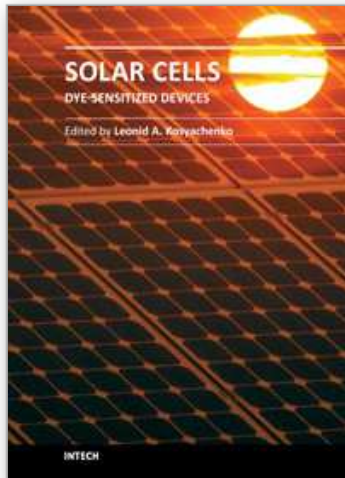
6. References

- Allegrucci, A., Lewcenko, N. A., et al. (2009). "Improved performance of porphyrin-based dye sensitised solar cells by phosphinic acid surface treatment." *Energy and Environmental Science*, Vol. 2, pp 1069.
- Armel, V., Pringle, J. M., et al. (2010). "Ionic liquid electrolyte porphyrin dye sensitised solar cells." *Chemical Communications*, Vol. 46, pp 3146.
- Bach, U., Lupo, D., et al. (1998). "Solid-state dye-sensitized mesoporous TiO₂ solar cells with high photon-to-electron conversion efficiencies." *Nature*, Vol. 395, pp 583.
- Barnes, P. R., Liu, L., et al. (2009). "Re-evaluation of recombination losses in dye-sensitized cells: the failure of dynamic relaxation methods to correctly predict diffusion length in nanoporous photoelectrodes." *Nano Letters*, Vol. 9, pp 3532.
- Bessho, T., Zakeeruddin, S. M., et al. (2010). "Highly efficient mesoscopic dye-sensitized solar cells based on donor-acceptor-substituted porphyrins." *Angewandte Chemie (International Edition)*, Vol. 49, pp 6646.
- Bisquert, J. & Mora-Sero, I. (2010). "Simulation of steady-state characteristics of dye-sensitized solar cells and the interpretation of the diffusion length." *Journal of Physical Chemistry Letters*, Vol. 1, pp 450.
- Boschloo, G. & Hagfeldt, A. (2009). "Characteristics of the iodide/triiodide redox mediator in dye-sensitized solar cells." *Accounts of Chemical Research*, Vol. 42,(11), pp 1819.
- Burke, A., Ito, S., et al. (2008). "The function of a TiO₂ compact layer in dye-sensitized solar cells incorporating "planar" organic dyes." *Nano Letters*, Vol. 8, pp 977.
- Campbell, W. M., Burrell, A. K., et al. (2004). "Porphyrins as light harvesters in the dye sensitized solar cell." *Coordination Chemistry Reviews*, Vol. 248, pp 1363.
- Campbell, W. M., Jolley, K. W., et al. (2007). "Zn porphyrins as highly efficient sensitizers in dye sensitized solar cells." *Journal of Physical Chemistry C*, Vol. 111, pp 11760.
- Chiba, Y., Islam, A., et al. (2006). "Dye sensitized solar cells with conversion efficiency of 11.1%." *Japanese Journal of Applied Physics*, Vol. 48, pp L638.
- Clifford, J. N., Forneli, A., et al. (2011). "Co-sensitized DSCs: dye selection criteria for optimized device V_{oc} and efficiency " *Journal of Materials Chemistry*, Vol. 21, pp 1693.
- Clifford, J. N., Palomares, E., et al. (2004). "Multistep electron transfer processes on dye co-sensitized nanocrystalline TiO₂ films." *Journal of the American Chemical Society*, Vol. 126, pp 5670.
- Clifford, J. N., Yahioğlu, G., et al. (2002). "Molecular control of recombination dynamics in dye sensitised nanocrystalline TiO₂ films." *Chemical Communications*, Vol., pp 1260.

- Dos Santos, T., Morandeira, A., et al. (2010). "Injection limitations in a series of porphyrin dye sensitized solar cells." *Journal of Physical Chemistry C*, Vol. 114, pp 3276.
- Fukai, Y., Kondo, Y., et al. (2007). "Highly efficient dye-sensitized SnO₂ solar cells having sufficient electron diffusion length " *Electrochemistry Communications*, Vol. 9, pp 1439.
- Furube, A., Katoh, R., et al. (2005). "Lithium ion effect on electron injection from a photoexcited coumarin derivative into a TiO₂ nanocrystalline film investigated by visible-to-IR ultrafast spectroscopy." *Journal of Physical Chemistry B*, Vol. 109, pp 16406.
- Geng, L. & Murray, R. W. (1986). "Oxidative microelectrode voltammetry of tetraphenylporphyrin and copper tetraphenylporphyrin in toluene solvent." *Inorganic Chemistry*, Vol. 25, pp 3115.
- Gledhill, S. E., Scott, B., et al. (2005). "Organic and nano-structured composite photovoltaics: An overview " *Journal Material Research*, Vol. 20, pp 3167.
- Gouterman, M. (1978). "Electronic Spectra", In: *The Porphyrins (Vol. III)*. D. Dolphin (ed.), Academic Press Inc., New York.
- Grätzel, M. (2001). "Photoelectrochemical cells." *Nature*, Vol. 414, pp 338.
- Grätzel, M. (2005). "Solar energy conversion by dye sensitized photovoltaic cells." *Inorganic Chemistry*, Vol. 44, pp 6841.
- Griffith, M. J., Mozer, A. J., et al. (2011). "Remarkable synergistic effects in a mixed porphyrin dye-sensitized TiO₂ film." *Applied Physics Letters*, Vol. 98, pp 163502.
- Guo, Q., Cocks, I., et al. (1997). "The orientation of acetate on a TiO₂(110) surface." *Journal of Physical Chemistry*, Vol. 106,(7), pp 2924.
- Haque, S. A., Palomares, E., et al. (2005). "Charge separation versus recombination in dye sensitized solar cells: The minimization of kinetic redundancy." *Journal of the American Chemical Society*, Vol. 127, pp 3456.
- Hara, K., Sato, T., et al. (2003). "Molecular design of coumarin dyes for efficient dye sensitized solar cells." *Journal of Physical Chemistry B*, Vol. 107, pp 597.
- Hardin, B. E., Hoke, E. T., et al. (2009). "Increased light harvesting in dye-sensitized solar cells with energy relay dyes." *Nature Photonics*, Vol. 3, pp 406.
- Hengerer, R., Kavan, L., et al. (2000). "Orientation dependence of charge-transfer processes on TiO₂ (anatase) single crystals." *Journal of the Electrochemical Society*, Vol. 147,(4), pp 1467.
- Hsieh, C.-P., Lu, H.-P., et al. (2010). "Synthesis and characterization of porphyrin sensitizers with various electron-donating substituents for highly efficient dye-sensitized solar cells." *Journal of Materials Chemistry*, Vol. 20, pp 1127.
- Imahori, H. (2010). "Porphyrins as potential sensitizers for dye sensitized solar cells." *Key Engineering Materials*, Vol. 451, pp 29.
- Imahori, H., Umeyama, T., et al. (2009). "Large π -aromatic molecules as potential sensitizers for highly efficient dye sensitized solar cells." *Accounts of Chemical Research*, Vol. 42, pp 1809.
- Kambe, S., Nakade, S., et al. (2002). "Influence of the electrolytes on electron transport in mesoporous TiO₂ electrolyte systems." *Journal of Physical Chemistry B*, Vol. 106, pp 2967.

- Katoh, R., Furube, A., et al. (2002). "Efficiencies of electron injection from excited sensitizer dyes to nanocrystalline ZnO films as studied by near-IR optical absorption of injected electrons." *Journal of Physical Chemistry B*, Vol. 106, pp 12957.
- Kay, A. & Grätzel, M. (1993). "Artificial photosynthesis. 1. Photosensitization of TiO₂ solar cells with chlorophyll derivatives and related natural porphyrins." *Journal of Physical Chemistry*, Vol. 97, pp 6272.
- Koehorst, R. B. M., Boschloo, G. K., et al. (2000). "Spectral sensitization of TiO₂ substrates by monolayers of porphyrin heterodimers." *Journal of Physical Chemistry B*, Vol. 104, pp 2371.
- Koops, S. E. & Durrant, J. R. (2008). "Transient emission studies of electron injection in dye sensitised solar cells." *Inorganica Chimica Acta*, Vol. 361, pp 8.
- Koumura, N., Wang, Z.-S., et al. (2006). "Alkyl-functionalized organic dyes for efficient molecular photovoltaics." *Journal of the American Chemical Society*, Vol. 128, pp 14256.
- Kuang, D., Ito, S., et al. (2006). "Stable mesoscopic dye-sensitized solar cells based on tetracyanoborate ionic liquid electrolyte." *Journal of the American Chemical Society*, Vol. 128, pp 4146.
- Lee, C.-W., Lu, H.-P., et al. (2009). "Novel zinc porphyrin sensitizers for dye sensitized solar cells: Synthesis and spectral, electrochemical, and photovoltaic properties." *Chemistry; A European Journal*, Vol. 15, pp 1403.
- Liu, C.-Y., Tang, H., et al. (1996). "Effect of orientation of porphyrin single crystal slices on optoelectronic properties." *Journal of Physical Chemistry*, Vol. 100, pp 3587.
- Liu, Y., Hagfeldt, A., et al. (1998). "Investigation of influence of redox species on the interfacial energetics of a dye-sensitized nanoporous TiO₂ solar cell " *Solar Energy Materials and Solar Cells*, Vol. 55, pp 267.
- Lo, C.-F., Hsu, S.-J., et al. (2010). "Tuning spectral and electrochemical properties of porphyrin-sensitized solar cells." *Journal of Physical Chemistry C*, Vol. 114, pp 12018.
- Marcus, R. A. (1964). "Chemical and electrochemical electron-transfer theory." *Annual Review of Physical Chemistry*, Vol. 15, pp 155.
- Martinson, A. B. F., Elam, J. W., et al. (2007). "ZnO nanotube based dye sensitized solar cells." *Nano Letters*, Vol. 8, pp 2183.
- Miyashita, M., Sunahara, K., et al. (2008). "Interfacial electron-transfer kinetics in metal-free organic dye sensitized solar cells: Combined effects of molecular structure of dyes and electrolytes." *Journal of the American Chemical Society*, Vol. 130, pp 17874.
- Mor, G. K., Shankar, K., et al. (2006). "Use of highly-ordered TiO₂ nanotube arrays in dye-sensitized solar cells." *Nano Letters*, Vol. 2, pp 215.
- Mori, S. & Asano, A. (2010). "Light intensity independent electron transport and slow charge recombination in dye-sensitized In₂O₃ solar cells: In contrast to the case of TiO₂." *Journal of Physical Chemistry C*, Vol. 114, pp 13113.
- Mori, S., Nagata, M., et al. (2010). "Enhancement of incident photon-to-current conversion efficiency for phthalocyanine-sensitized solar cells by 3D molecular structuralization." *Journal of the American Chemical Society*, Vol. 132, pp 4054.
- Mozer, A. J., Griffith, M. J., et al. (2009). "Zn-Zn porphyrin dimer-sensitized solar cells: Towards 3-D light harvesting." *Journal of the American Chemical Society*, Vol. 131,(43), pp 15621.

- Mozer, A. J., Wagner, P., et al. (2008). "The origin of open circuit voltage of porphyrin-sensitized TiO₂ solar cells." *Chemical Communications*, Vol., pp 4741.
- Nakade, S., Kanzaki, T., et al. (2005). "Role of electrolytes on charge recombination in dye-sensitized TiO₂ solar cell (1): The case of solar cells using the I⁻/I₃⁻ redox couple." *Journal of Physical Chemistry B*, Vol. 109, pp 3480.
- Nazeeruddin, M. K., Pechy, P., et al. (2001). "Engineering of efficient panchromatic sensitizers for nanocrystalline TiO₂-based solar cells." *Journal of the American Chemical Society*, Vol. 123, pp 1613.
- Nogueira, A. F. & Paoli, M.-A. D. (2001). "Electron transfer dynamics in dye sensitized nanocrystalline solar cells using a polymer electrolyte." *Journal of Physical Chemistry B*, Vol. 105, pp 7517.
- O'Regan, B. & Grätzel, M. (1991). "A low-cost, high-efficiency solar cell based on dye-sensitized colloidal TiO₂ films." *Nature*, Vol. 353, pp 737.
- O'Regan, B. C., Durrant, J. R., et al. (2007). "Influence of the TiCl₄ treatment on nanocrystalline TiO₂ films in dye-sensitized solar cells. 2. Charge density, band edge shifts, and quantification of recombination losses at short circuit." *Journal of Physical Chemistry C*, Vol. 111, pp 14001.
- O'Regan, B. C., López-Duarte, I., et al. (2008). "Catalysis of recombination and its limitation on open circuit voltage for dye sensitized photovoltaic cells using phthalocyanine dyes." *Journal of the American Chemical Society*, Vol. 130, pp 2906.
- Planells, M., Forneli, A., et al. (2008). "The effect of molecular aggregates over the interfacial charge transfer processes on dye sensitized solar cells." *Applied Physics Letters*, Vol. 92, pp 153506.
- Sauvé, G., Cass, M. E., et al. (2000). "Dye sensitization of nanocrystalline titanium dioxide with osmium and ruthenium polypyridyl complexes." *Journal of Physical Chemistry B*, Vol. 104, pp 6821.
- Shaheen, S. E., Ginley, D. S., et al. (2005). "Organic Based Photovoltaics: Towards Lower Cost Power Generation." *MRS Bulletin*, Vol. 20, pp 10.
- Shockley, W. & Queisser, H. J. (1961). "Detailed balance limit of efficiency of p-n junction solar cells." *Journal of Applied Physics*, Vol. 32, pp 510.
- Wagner, K., Griffith, M. J., et al. (2011). "Significant performance improvement of porphyrin-sensitized TiO₂ solar cells under white light illumination." *Journal of Physical Chemistry C*, Vol. 115, pp 317.
- Wang, P., Zakeeruddin, S. M., et al. (2003). "A new ionic liquid electrolyte enhances the conversion efficiency of dye sensitized solar cells." *Journal of Physical Chemistry B*, Vol. 107, pp 13280.
- Westermarck, K., Rensmo, H., et al. (2002). "PES studies of Ru(dcbpyH₂)₂(NCS)₂ adsorption on nanostructured ZnO for solar cell applications." *Journal of Physical Chemistry B*, Vol. 106, pp 10102.
- Willis, R. L., Olson, C., et al. (2002). "Electron dynamics in nanocrystalline ZnO and TiO₂ films probed by potential step chronoamperometry and transient absorption spectroscopy." *Journal of Physical Chemistry B*, Vol. 106, pp 7605.
- Zaban, A., Ferrere, S., et al. (1998). "Relative energetics at the semiconductor/sensitizing dye/electrolyte interface." *Journal of Physical Chemistry B*, Vol. 102, pp 452.
- Zheng, H., Tachibana, Y., et al. (2010). "Dye sensitized solar cells based on WO₃." *Langmuir*, Vol. 26, pp 19148.



Solar Cells - Dye-Sensitized Devices

Edited by Prof. Leonid A. Kosyachenko

ISBN 978-953-307-735-2

Hard cover, 492 pages

Publisher InTech

Published online 09, November, 2011

Published in print edition November, 2011

The second book of the four-volume edition of "Solar cells" is devoted to dye-sensitized solar cells (DSSCs), which are considered to be extremely promising because they are made of low-cost materials with simple inexpensive manufacturing procedures and can be engineered into flexible sheets. DSSCs are emerged as a truly new class of energy conversion devices, which are representatives of the third generation solar technology. Mechanism of conversion of solar energy into electricity in these devices is quite peculiar. The achieved energy conversion efficiency in DSSCs is low, however, it has improved quickly in the last years. It is believed that DSSCs are still at the start of their development stage and will take a worthy place in the large-scale production for the future.

How to reference

In order to correctly reference this scholarly work, feel free to copy and paste the following:

Matthew J. Griffith and Attila J. Mozer (2011). Porphyrin Based Dye Sensitized Solar Cells, Solar Cells - Dye-Sensitized Devices, Prof. Leonid A. Kosyachenko (Ed.), ISBN: 978-953-307-735-2, InTech, Available from: <http://www.intechopen.com/books/solar-cells-dye-sensitized-devices/porphyrin-based-dye-sensitized-solar-cells>

INTECH
open science | open minds

InTech Europe

University Campus STeP Ri
Slavka Krautzeka 83/A
51000 Rijeka, Croatia
Phone: +385 (51) 770 447
Fax: +385 (51) 686 166
www.intechopen.com

InTech China

Unit 405, Office Block, Hotel Equatorial Shanghai
No.65, Yan An Road (West), Shanghai, 200040, China
中国上海市延安西路65号上海国际贵都大饭店办公楼405单元
Phone: +86-21-62489820
Fax: +86-21-62489821

© 2011 The Author(s). Licensee IntechOpen. This is an open access article distributed under the terms of the [Creative Commons Attribution 3.0 License](#), which permits unrestricted use, distribution, and reproduction in any medium, provided the original work is properly cited.

IntechOpen

IntechOpen